

## Temperature fluctuation properties in sodium convection

S. Cioni,\* S. Horanyi,† L. Krebs, and U. Müller‡

Forschungszentrum Karlsruhe GmbH, Institut für Angewandte Thermo und Fluidodynamik, Postfach 3640,  
D-76021 Karlsruhe 1, Germany

(Received 9 December 1996)

Experimental investigations have been carried out on some aspects of temperature field in sodium convection. Using spectra, histograms, and structure functions the properties of the temperature fluctuations were analyzed. It was found that, at  $Ra \approx 5 \times 10^6$ , the maximum Rayleigh number reached in this experiment, the temperature field behavior was mainly diffusive. The frequency spectra showed a very clear scaling with a slope of  $-4$ . It was also found that, over the whole range of Rayleigh numbers checked, the probability density functions (PDF's) of the temperature fluctuations were Gaussian shaped, whereas the PDF's of the temperature differences were well fitted by stretched exponential tails. [S1063-651X(97)51009-9]

PACS number(s): 47.27.Te

Rayleigh-Bénard convection, a fluid layer heated from below and cooled from above, has been studied for a long time. The majority of this work has been devoted to the large Prandtl number fluids in different geometries. A few numbers of studies have dealt with the low Prandtl number flow ([1–3]). While earlier studies focused on the global heat transfer and flow patterns, more recent interest arised in the statistical properties of turbulence ([4]). A new regime of turbulence, corresponding to the Bolgiano-Obukhov scaling, seems to occur at moderate Prandtl number [4,5]. By contrast, experiments in mercury [6] suggest that temperature fluctuations are passively transported by turbulence at low Prandtl number, in agreement with theoretical expectations [7].

Thus, the main aim of this paper is to characterize the moderate Rayleigh number regime at a very low Prandtl number ( $Pr \approx 5 \times 10^{-3}$ ) [8]. In order to do this, the properties of the turbulence regime have been characterized by means of various statistical quantities such as histograms, frequency power spectra and structure functions of local temperature fluctuations. In this paper, we will study the temperature field for different Rayleigh numbers at different locations inside the cell.

The experimental setup has been detailed in Horanyi *et al.* [9] (see also [1]). Here, we give only the main features. The experimental cell was a vertical cylinder 110 mm high and 520 mm in diameter, corresponding to the aspect ratio  $\Gamma = D/H = 4.72$ .

The control parameter of this experiment was the heating power. Thus, the experimental boundary conditions were fixed heat flux at the bottom and fixed temperature at the top.

The mean working temperature was 570 K [10] and the Rayleigh number ranged from  $2 \times 10^5$  to  $5 \times 10^6$ .

The measurements presented in the present paper were obtained from two rake probes near the center as shown in Fig. 1. Each rake consisted of nine thermocouples spanning from the bottom to the top plate as shown in Fig. 1(b). We shall focus on the results at 15 mm from the top plate, as the presence of the mean flow allows us to relate the time domain to the spatial one by means of the Taylor hypothesis (for further details on the flow pattern inside the cell as well as on the heat flux measurements, see [9]). Furthermore, the data presented here were obtained using a  $5 \times 10^4$  data set sampled at 10 Hz, which corresponds to 100 times the turn over time (see below).

The study of the shape of the probability density functions (PDF's) is related to the problem of intermittency, which is a fundamental problem in turbulence (see Ching [11] for application to the Rayleigh-Bénard convection). In fact, intermittency in space and time is responsible for the deviation from the Gaussian statistics.

In Fig. 2(a) we show a temperature fluctuation time series and the corresponding PDF at  $Ra \approx 1.5 \times 10^6$  [12], taken at a distance  $H/8$  from the top plate, corresponding to  $z/\lambda_{th} \approx 1$

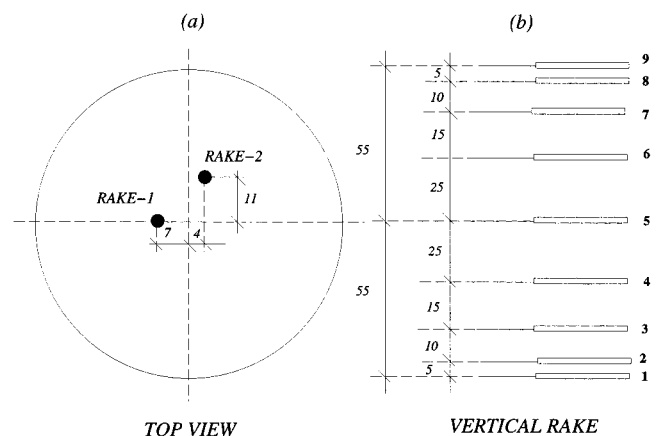


FIG. 1. (a) Schematic drawing of one plate (top view). The dots indicate the horizontal location of the two vertical rakes. (b) Each rake consisted of nine thermocouples. Quotas are in mm.

\*Author to whom correspondence should be addressed. Present address: Ecole Normale Supérieure de Lyon, Laboratoire de Physique, 46, Allée d'Italie 69364 Lyon Cedex 07, France. Electronic address: scioni@physique.ens-lyon.fr

†Present address: Central Research Institut for Physics, Atomic Energy Institut, P.O. Box 49, H-1525 Budapest, Hungary. Electronic address: horanyi@ifk.kfki.hu

‡Electronic address: mueller@iatf.fzk.de

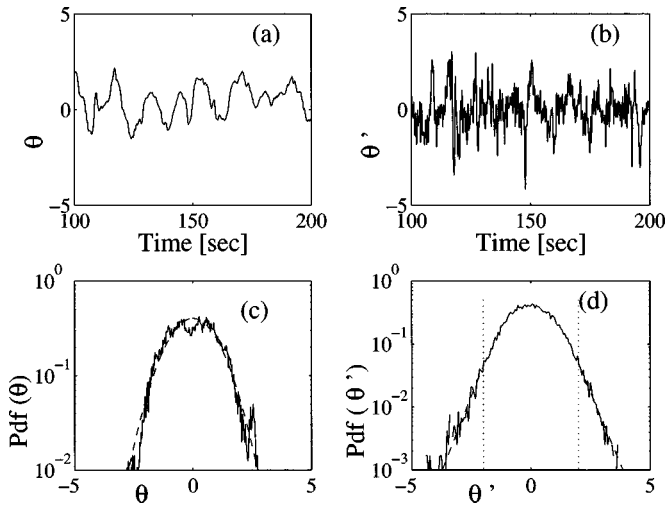


FIG. 2. (a) Typical time recording of the temperature fluctuations normalized by the root-mean-squared  $\Delta_c$  and (c) the corresponding PDF  $P(\theta)$  with  $\theta = (T - \langle T \rangle) / \Delta_c$  at  $H/8$  from the top boundary for  $Ra = 1.5 \times 10^6$ . The dashed line in (c) represents the Gaussian distribution. (b) Time derivative and (d) the corresponding PDF at the same Rayleigh number, where  $\theta' = (\partial T / \partial t) / (\langle \partial T / \partial t \rangle)^{1/2}$ . The dashed lines in (d) represent the fit by a stretched-exponential tiles, with  $\beta = 1$  for  $|\theta| > 2$  (see text).

[12]. In order to calculate the time derivative  $\partial T / \partial t$  from the digitalized temperature fluctuations  $T_i$  we estimate the time derivative using a centered difference [13]

$$dT_i = \frac{(T_{i+1} - T_{i-1}))}{2},$$

and divide by the sampling time step  $\Delta t = 0.1$  sec [see Fig. 2(b)].

The normalized PDF of the temperature fluctuations and of its derivatives are shown in Figs. 2(c) and 2(d), respectively. The dashed line represents the Gaussian distribution with the same mean standard deviation as the turbulent signal [Fig. 2(c)]. As can be seen from Fig. 2(c), the histogram

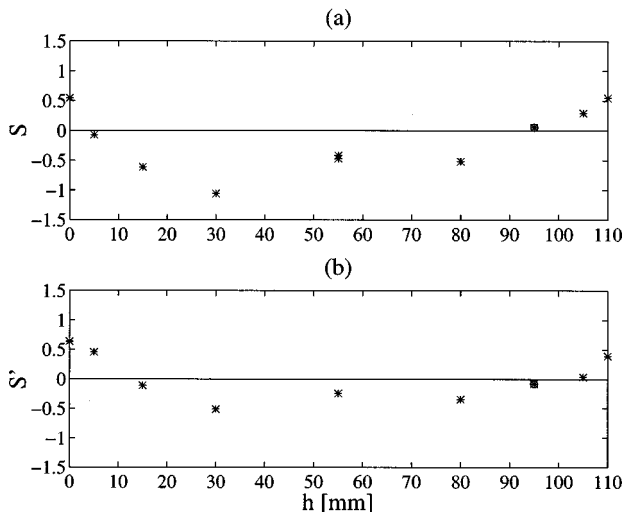


FIG. 3. Skewness of the temperature fluctuations (a) and its derivatives (b) at  $Ra \approx 1.6 \times 10^6$  versus height. The circle-star point corresponds to the location of the results shown in this paper.

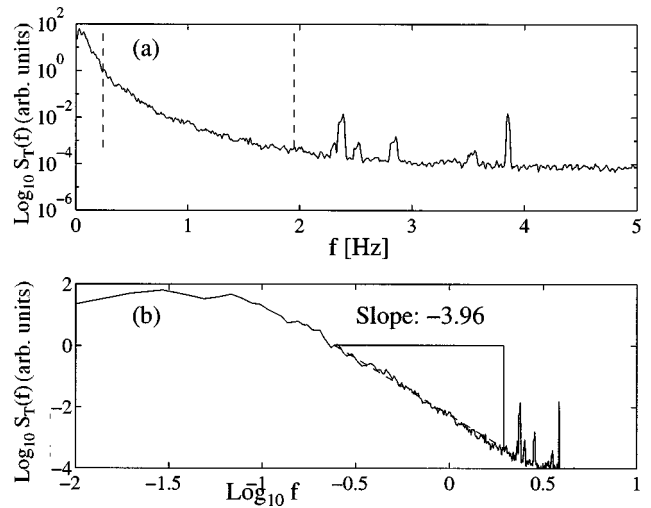


FIG. 4. Frequency spectrum of temperature fluctuations at  $Ra = 1.5 \times 10^6$  and  $h = 95$  mm (a) Log-log plot; (b) log-lin plot. The two vertical dashed lines correspond to the fit region.

is very close to the Gaussian distribution, verifying that turbulence has not fully developed. On the other hand, the PDF's of temperature differences is well fitted by a stretched-exponential form [11]

$$\rho(\theta) = \rho(0) e^{-c|\theta|^\beta}, \quad c, \beta > 0.$$

Note that  $\beta = 2$  corresponds to Gaussian distribution and  $\beta = 1$  corresponds to exponential distribution, while  $\beta < 1$  indicates a flatter intermittent distribution.

At that location these PDF's are symmetric, the corresponding skewness factors [14]  $S$  and  $S'$  respectively, for the fluctuations and its derivatives are,  $S = 0.055$  and  $S' = -0.079$ . Figure 3 shows the skewness factors  $S$  and  $S'$  as functions of the cell's height. Similar results have been obtained by Belmonte and Libchaber [13] but at moderate Prandtl number and larger Rayleigh number.

The spectra of temperature fluctuations provide a further test for the characterization of the turbulent regime. As emphasized by Chasnov *et al.* [15], there are few published contributions that bear directly on the problem of the temperature field behavior in turbulent fluid at low Prandtl number. Also, given the variety of theoretically published laws (i.e., exponential,  $-17/3$ ,  $-13/3$ , and  $-3$ ), the problem of scal-

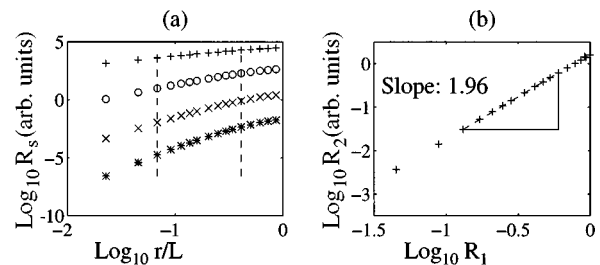


FIG. 5. Log-log plot of  $R_s$  vs  $r/L$  at  $Ra \approx 1.6 \times 10^6$ . The symbols are +,  $s = 1$ ;  $\circ$ ,  $s = 2$ ;  $\times$ ,  $s = 3$ ;  $*$ ,  $s = 4$ . Curves have been vertically shifted by +5 ( $s = 1$ ), +5 ( $s = 1$ ), +2.5 ( $s = 2$ ), 0 ( $s = 3$ ), -2.5 ( $s = 4$ ). The vertical dashed lines represent the fit range of the scaling exponents given in Table I (see text). (b) Log-log plot of  $R_2$  vs  $R_1$ .

TABLE I. Scaling exponent for the temperature structure functions  $R_s$  where  $s$  is the order.

	$s=1$	$s=2$	$s=3$	$s=4$	$s=5$	$s=6$
$\xi_s$	0.86	1.67	2.42	3.09	3.70	4.26
$\epsilon_s^a$	$\pm 0.01$	$\pm 0.03$	$\pm 0.04$	$\pm 0.05$	$\pm 0.08$	$\pm 0.09$

<sup>a</sup> $\epsilon_s$  represent the error bars.

ing behavior in the conductive subrange still awaits an answer. It is well known [16] that for Prandtl numbers less than 1 the temperature fluctuations spectra in the conductive range for a passive scalar are given by the relation  $S_T(k) \sim S_V(k)k^{-4}$ , where  $S_V$  is the velocity spectrum.

Using the mean velocity (computed from the correlation between two probes (see [4] and [9]) we can relate the time domain with the spatial one. The mean velocity measured at  $Ra=1.5 \times 10^6$  was  $V \approx 2.5$  cm/sec. Figure 4 shows the frequency power spectrum for  $Ra \approx 1.5 \times 10^6$  at 15 mm from the top plate. The log-lin plot of Fig. 4(a) shows clearly that the spectrum can best be fitted by a power law than by an exponential one. In fact, the log-log plot [see Fig. 4(b)] is well fitted with a power exponent equal to  $f_L \approx -3.96$ . The latter ranges from 0.24 Hz (corresponding to the integral scale  $L \approx V/f_L$ ) to 2.0 Hz.

This means that at this Rayleigh number, neither the so-called inertial-convective subrange (characterized by a  $k^{-5/3}$  spectrum) nor (for larger  $k$ ) the so-called inertial-conductive subrange (characterized by a Batchelor spectrum in  $\sim k^{-17/3}$  [17]) were observed. Thus, there is a range of wave numbers (read frequency)  $k$  for which the velocity spectrum is *constant* while fluctuations for the temperature field are in their *conductive* range. The reason for this could be found in the fact that as the Reynolds number was not high enough to develop any ‘inertial’ subrange, the temperature spectrum fell off before the viscous cut-off could occur.

Furthermore, the spectra at 1.5 cm as well as in the middle of the cell were perfectly superimposable. This means that at this Rayleigh number the whole layer of sodium was dominated by diffusive effects. It is of interest to examine whether this dissipative scaling can be observed even from the structure functions.

The structure function  $R_s$ , of order  $s$ , is defined by the following relationship:

$$R_s(r) = \langle |T(x+r) - T(x)|^s \rangle = \langle |\delta T(r)|^s \rangle.$$

Figure 5(a) shows  $R_s$  versus  $r$  for  $s=1,2,3,4$  corresponding to the turbulent signal given in Fig. 2. We should stress the excellent agreement between the estimation of the mean velocity and the fact that the structure functions become flat for  $r/L=1$ , as commonly observed in ordinary turbulence. The best fit of  $R_s$  over the range indicated by the vertical dashed lines of Fig. 5(a) gives the scaling exponents reported in Table I.

A more effective way of studying the turbulence regime is provided by the extended self-similarity (ESS) introduced by Benzi *et al.* in 1993 [18]. As pointed out by Benzi *et al.*, if we suppose that the temperature structure functions of order  $s$  follow a scaling law of this kind,

$$R_s(r) \sim r^{\xi_s},$$

the  $s$ -order structure function versus the  $t$ -order structure function has to follow the following scaling:

$$\frac{R_s}{R_t} \sim r^{\Delta(s,t)},$$

where

$$\Delta(s,t) = \frac{\xi_s}{\xi_t}$$

is the so-called *self-exponent* for the temperature field.

ESS supports previous conclusions inferred from the frequency spectra. In fact, Fig. 5 shows that as the self-exponent  $\Delta(2,1)$  is equal to  $-1.98$ , the temperature field is fully conductive [remember that in the dissipative range,  $\Delta(s,t) = s/t$ ].

In this paper some properties of the temperature structure field have been investigated experimentally. The results of the present investigation have demonstrated that the temperature field at these Rayleigh numbers in sodium liquid was purely dissipative: the Gaussian distribution of the PDF proves this. Furthermore, a regime characterized by a  $f^{-4}$  scaling law in the temperature fluctuation spectra has been observed experimentally.

[1] V. Kek and U. Muller, *Int. J. Heat Mass Transf.* **36**, 2795 (1993).  
 [2] S. Globe and D. Dropkin, *Int. J. Heat Mass Transf.* **31**, 24 (1959); H. T. Rossby, *J. Fluid Mech.* **36**, 309 (1969); T. Takeshita, T. Segawa, J. A. Glazier, and M. Sano, *Phys. Rev. Lett.* **76**, 1465 (1996).  
 [3] S. Cioni, S. Ciliberto, and J. Sommeria, *Dyn. Atmos. Oceans* **24**, 117 (1996); S. Cioni *et al.*, *J. Fluid Mech.* **73**, 693 (1997).  
 [4] F. Heslot, B. Castaing, and A. Libchaber, *Phys. Rev. A* **36**, 5870 (1987); M. Sano, X. Z. Wu, and A. Libchaber, *ibid.* **40**, 6421 (1989); X. Wu, L. Kadanoff, A. Libchaber, and M. Sano, *Phys. Rev. Lett.* **64**, 2140 (1990).

[5] R. Benzi, R. Tripiccion, F. Massaioli, S. Succi, and S. Ciliberto, *Europhys. Lett.* **25**, 341 (1994).  
 [6] S. Cioni, S. Ciliberto, and J. Sommeria, *Europhys. Lett.* **32**, 413 (1995).  
 [7] E. Siggia, *Annu. Rev. Fluid Mech.* **26**, 137 (1994).  
 [8] The Rayleigh number is defined as  $Ra = g\alpha\Delta L^3/\nu\kappa$ , where  $g$  is the gravitational acceleration,  $L$  the height of the cell,  $\Delta$  the temperature difference,  $\alpha$  the thermal expansion coefficient of the fluid,  $\nu$  its kinematic viscosity, and  $\kappa$  its thermal diffusivity. The Prandtl number is equal to  $Pr = \nu/\kappa$ .  
 [9] S. Horanyi, L. Krebs, and U. Müller (unpublished).  
 [10] At this temperature typical values of the physical properties of

sodium are  $\kappa \approx 6.6 \times 10^{-5}$  m<sup>2</sup>/sec,  $\alpha \approx 3 \times 10^{-4}$  1/K,  $\nu \approx 3.8 \times 10^{-7}$  m<sup>2</sup>/sec.

- [11] E. S. C. Ching, Phys. Rev. E **44**, 3622 (1991).
- [12] At this Rayleigh number the corresponding temperature difference  $\Delta$  was 10 K and the Nusselt number was 3.9, which corresponds, approximately, to a thermal boundary thickness of  $\lambda_{th} \approx L/2Nu \approx 15$  mm, where Nusselt is the nondimensional convective heat flux defined as the ratio of the total heat flux over the conductive heat flux.
- [13] A. Belmonte and A. Libchaber, Phys. Rev. E **53**, 4893 (1996).
- [14] The skewness  $S$  and  $S'$  are defined respectively by the following relations:  $S = \langle (T - \langle T \rangle)^3 \rangle / \langle (T - \langle T \rangle)^2 \rangle^{3/2}$  and  $S' = \langle (\partial T / \partial t)^3 \rangle / \langle (\partial T / \partial t)^2 \rangle^{3/2}$ .
- [15] J. Chasnov, V. M. Canuto, and R. S. Rogallo, Phys. Fluids **31**, 2065 (1988).
- [16] M. Lesieur, *Turbulence in Fluids* (Martinus Nijhoff Publishers, Boston, 1987), p. 142.
- [17] G. K. Batchelor, I. D. Howells, and A. A. Townsend, J. Fluid Mech. **5**, 134 (1959).
- [18] R. Benzi, S. Ciliberto, R. Tripiccone, C. Baudet, F. Massaioli, and S. Succi, Phys. Rev. E **48**, 29 (1993).